

Stark-level one-phonon dephasing process of Nd³⁺-doped silicate glass fiber studied with accumulated photon echoes

Ryuzi Yano and Naoshi Uesugi

NTT Basic Research Laboratories, 3-1, Morinosato-Wakamiya, Atsugi-shi, Kanagawa, 243-01, Japan

(Received 27 February 1996; revised manuscript received 2 August 1996)

Measurements of the homogeneous width of the ${}^4G_{5/2}$, ${}^2G_{7/2}$ - ${}^4I_{9/2}$ transition of Nd³⁺ in a silicate glass fiber at low temperatures by the technique of accumulated photon echoes show that the dephasing processes are one-phonon processes between the Stark levels of Nd³⁺. These dephasing processes differ from the commonly observed processes of rare-earth ion-doped glasses: the local-configurational-change-induced dephasing process and the Raman process with low-frequency modes. The densely distributed Stark levels of the ${}^4G_{5/2}$ and ${}^2G_{7/2}$ states are responsible for one-phonon processes. The transition-wavelength dependences of the homogeneous widths $\Gamma_h(4.2\text{ K})$ and $\Gamma_h(T \rightarrow 0)$ are explained by using the one-phonon process model. [S0163-1829(97)03609-6]

I. INTRODUCTION

Many studies have been performed to clarify the mechanism of the anomalous optical properties of ion-doped glasses from the viewpoints of pure and applied sciences.¹ In a recent study of the accumulated photon echoes,² we have measured the temperature dependence of the homogeneous width of the 5D_0 - 7F_0 transition of Eu³⁺ (Ref. 3) and of the ${}^4F_{3/2}(1)$ - ${}^4I_{9/2}$ transition of Nd³⁺ (Ref. 4) when both ions were doped in a pure silicate glass fiber at low temperatures. Both the temperature dependences showed a crossover from T linear ($T < 7\text{ K}$) to T^2 ($T > 7\text{ K}$, Ref. 7). The dephasing processes could be well explained by the two-level system (TLS) dephasing process¹ and the Raman process with low-frequency modes.^{5,16} A TLS models a local configurational change in glasses.^{1,6} These two dephasing processes are considered to be relevant to ion-doped inorganic glasses as the thermally nonequilibrium nature of the structure and the low-frequency modes are peculiar to glasses.⁶

The dephasing processes of the ${}^4G_{5/2}$, ${}^2G_{7/2}$ - ${}^4I_{9/2}$ transition of Nd³⁺ ions in ordered and disordered crystals [LaF₃ (Ref. 8) and CaF₂-YF₃ (Ref. 9)] at low temperatures have been considered to be one-phonon processes¹⁰ between the Stark levels of the ions. On the other hand, the homogeneous width of the ${}^4F_{3/2}(1)$ - ${}^4I_{9/2}$ transition of Nd³⁺ in a silicate glass fiber between 1.6 and 44 K has been explained by the TLS dephasing process and the Raman process with low-frequency modes.⁴ Obvious differences between the two transitions are the energy-level distributions of the excited states. The Stark levels of the ${}^4G_{5/2}$ and ${}^2G_{7/2}$ states are densely distributed, whereas the ${}^4F_{3/2}(1)$ state is a single state. Here arises a question. What is the dominant dephasing process of the ${}^4G_{5/2}$, ${}^2G_{7/2}$ - ${}^4I_{9/2}$ transition of Nd³⁺ at low temperatures when Nd³⁺ is doped into inorganic glass such as silicate glass?

The transition-wavelength dependence of the homogeneous width of the ${}^4G_{5/2}$, ${}^2G_{7/2}$ - ${}^4I_{9/2}$ transition of the Nd³⁺ ion-doped silicate glass (Hoya No. 5010) at 13 K was measured and the dephasing mechanism of this transition was, as explained in Ref. 11, attributed to the one-phonon processes.

There are, however, some ambiguities in that attribution. Since the temperature dependence of the homogeneous width was not measured, it was not possible to clearly discuss the dephasing mechanism of this transition.

In this paper we report experiments on accumulated photon echoes for the ${}^4G_{5/2}$, ${}^2G_{7/2}$ - ${}^4I_{9/2}$ transition of Nd³⁺ in a pure silicate glass fiber at low temperatures. Several dephasing mechanisms are discussed and the most probable dephasing mechanism is attributed to the one-phonon processes between the Stark levels of Nd³⁺. The transition-wavelength dependences of the homogeneous widths $\Gamma_h(4.2\text{ K})$ and $\Gamma_h(T \rightarrow 0)$ are well explained by the one-phonon process model.

II. EXPERIMENT

The experimental setup for the accumulated photon echoes is shown in Fig. 1. The excitation source was a mode-locked dye laser with a repetition rate of 82 MHz and a pulse width of 4 psec. The output of the laser was divided by a polarized beam splitter. An optical chopper modulated both

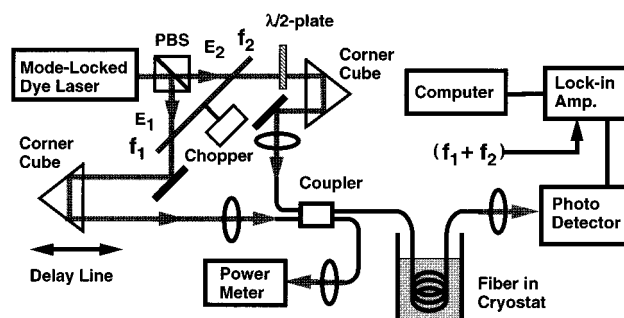


FIG. 1. Experimental setup for accumulated photon echoes using a mode-locked dye laser to measure the homogeneous widths of the ${}^4G_{5/2}$, ${}^2G_{7/2}$ - ${}^4I_{9/2}$ transition of Nd³⁺ in a pure silicate glass fiber. The intensities of the pump and probe beams E_1 and E_2 were modulated by an optical chopper. The heterodyne-detected echo signal was measured by changing the delay time t_{12} between the pump and probe beams.

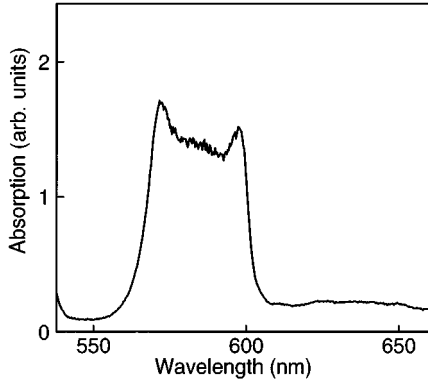


FIG. 2. Absorption spectrum of Nd^{3+} in a pure silicate glass fiber at 78 K.

the pump (E_1) and probe (E_2) beams at frequencies f_1 of 1.0 kHz and f_2 of 0.83 kHz. After a suitable delay of the probe beam, both the pump and probe beams were combined by a beam coupler (SIFAM; P22S63B50) and guided to the fiber sample. The $(f_1 + f_2)$ frequency component of the output beams from the fiber sample was detected by a lock-in amplifier.

Echo decay curves were measured by changing the delay time t_{12} between the pump and probe beams. Since the echo field was detected by heterodyne detection, the decay constant of the echo decay curve gave $T_2/2$,² where T_2 is the dephasing time. The homogeneous width Γ_h is given by $\Gamma_h = 1/(\pi T_2)$.

The input beam ratio of the pump and probe beams was set to about 3:1, and typical input intensities of the pump and probe beams were, respectively, 0.84 and 0.30 mW. When the input pump beam intensity was between 0.30 and 3.0 mW, the measured T_2 values were the same within experimental error.

The sample was a pure silicate glass single-mode fiber (cutoff wavelength of 780 nm) doped with 20 ppm Nd^{3+} . The 2.8-m-long fiber sample was coiled in a cage to a diameter of 4 cm. Nondoped single-mode fibers for 515 nm spliced onto both ends of the Nd^{3+} fiber sample were used to guide the excitation beams into and out of the cryostat. Below 4.2 K, the sample temperature was maintained within ± 0.1 K, and above 4.2 K, it was maintained within ± 0.2 K.³ At 78 K, the transmission loss for 595 nm was 3.6 dB/m.

If the wavelength of the excitation beams were shorter than the cutoff wavelength of the fiber sample, multimode coupling of the laser beam with the fiber is possible. The transverse mode of the pump beam (E_1) would have changed as the delay time t_{12} was changed. The change of the transverse mode would have made echo signals very noisy. As shown in the next section, however, we were able to obtain a clear echo decay curve, probably because the nondoped single-mode fiber purified the spatial mode structure of the exciting beams.

III. EXPERIMENTAL RESULTS AND DISCUSSION

The absorption spectrum of the Nd^{3+} fiber sample measured at 78 K is shown Fig. 2. No clear profile of the Stark levels is observed. Since the population excited to these

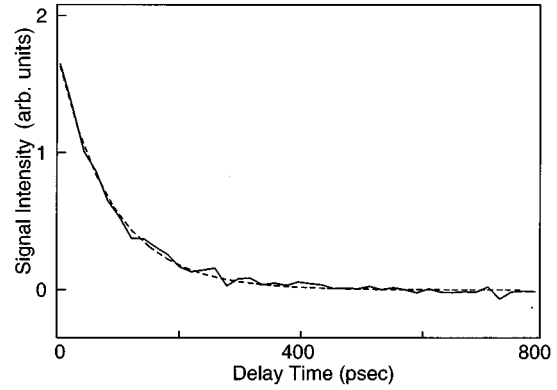


FIG. 3. Accumulated echo decay curve at 596 nm and 4.2 K. The dotted curve is a single exponential fitting with T_2 of 180 psec.

Stark levels emits phonons and relaxes to the lowest of the Stark level, we cannot obtain the Stark levels energy structure.

Figure 3 shows an echo decay curve measured at 596 nm and 4.2 K. The dashed curve is a theoretical fitting with T_2 of 180 psec, and assuming a single exponential decay. The agreement between the fitting and the measured data shows that the echo decay curve can be assumed to be a single exponential decay curve. We therefore approximated all the measured echo decay curves as single exponential decay curves.

Shelby observed double exponential echo decay curves at shorter wavelengths ($\lambda < 585$ nm) in Nd^{3+} :ED-2 silicate glass.¹² We observed, however, only single exponential decay curves. This is due to the fact that since we measured echo decay curves at $t_{12} > 10$ psec because of the collinear excitation beam configuration, we could not measure a faster decay components corresponding to $\Gamma_h > 40$ GHz.

Figures 4–6 show (a) the homogeneous widths $\Gamma_h(T)$'s measured at 590, 593, and 598 nm and (b) the temperature-dependent parts of these homogeneous widths $\Delta\Gamma_h(T)$'s:

$$\Delta\Gamma_h(T) = \Gamma_h(T) - \langle\Gamma_h(0)\rangle. \quad (1)$$

Here $\langle\Gamma_h(0)\rangle$'s are average values of the homogeneous widths in the temperature-independent region which for 590, 593, and 598 nm are, respectively, 2.2, 1.7, and 1.3 GHz. For

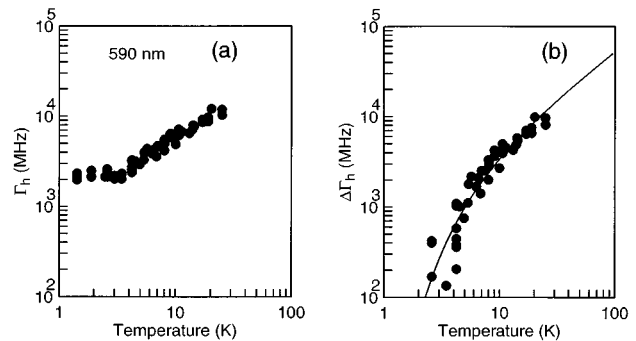


FIG. 4. Temperature dependence of (a) the measured homogeneous width of the ${}^4G_{5/2}, {}^2G_{7/2} \rightarrow {}^4I_{9/2}$ transition of Nd^{3+} at 590 nm and (b) the temperature-dependent part of that width. The curve is a theoretical fitting assuming a one-phonon process.

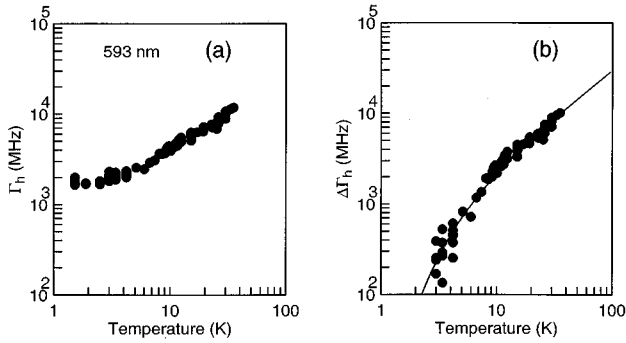


FIG. 5. Temperature dependence of (a) the measured homogeneous width of the ${}^4G_{5/2}$, ${}^2G_{7/2}$ - ${}^4I_{9/2}$ transition of Nd^{3+} at 593 nm and (b) the temperature-dependent part of that width. The curve is a theoretical fitting assuming a one-phonon process.

590 and 593 nm $\Delta\Gamma_h(T)$ is nearly proportional to T linear, and for 598 nm it is proportional to $T^{1.4}$ when $T > 6$ K. Below 6 K the temperature dependence of the $\Delta\Gamma_h(T)$'s becomes steeper than T linear or $T^{1.4}$. Because the measured $\Delta\Gamma_h(T)$'s have experimental errors, we use mainly the values at $T > 6$ K for the discussion of the dephasing mechanism.

In the following, we discuss the possible dephasing mechanisms of the homogeneous width of the ${}^4G_{5/2}$, ${}^2G_{7/2}$ - ${}^4I_{9/2}$ transition of the Nd^{3+} sample. The Raman process of the Debye model with acoustic phonons¹⁰ can be excluded because the temperature dependence of that process is steeper than T^2 at $T < T_D/2 = 247$ K,¹⁰ where T_D is the Debye temperature of silicate glass. Similarly, the Raman process with low-frequency modes can be excluded because its temperature dependence is steeper than T^2 at $T < 40$ K.⁵

First we consider the possibility of the TLS dephasing process and the Raman process with low-frequency modes peculiar to glasses.^{3,4} The theory of the TLS dephasing process predicts that the homogeneous width Γ_h is proportional to $T^{1+\mu}$ if the density of the TLS's $\rho(E) \propto E^\mu$.¹ Since a T -linear temperature dependence for the ${}^4F_{3/2}(1)$ - ${}^4I_{9/2}$ transition of Nd^{3+} in silicate glass fiber has already been observed,⁴ we assume that the temperature dependence of the TLS dephasing process for the measured transition is also T linear. The contributions of the TLS dephasing process and

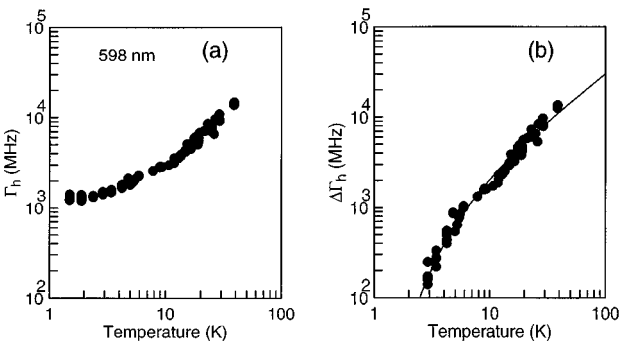


FIG. 6. Temperature dependence of (a) the measured homogeneous width of the ${}^4G_{5/2}$, ${}^2G_{7/2}$ - ${}^4I_{9/2}$ transition of Nd^{3+} at 598 nm and (b) the temperature-dependent part of that width. The curve is a theoretical fitting assuming a one-phonon process.

the Raman process with low-frequency modes can, respectively, be written as AT and $BF(T)$. Here, $F(T) \propto T^2$ at $T > 40$ K and changes more rapidly than T^2 at $T < 40$ K, and is defined as $F(T = 10 \text{ K}) = 1$ (no dimension).⁵ A and B are fitting parameters. The AT and $BF(T)$ functions were used previously for the discussion of the dephasing mechanisms of the homogeneous width of the 5D_0 - 7F_0 transition of Eu^{3+} and of the ${}^4F_{3/2}(1)$ - ${}^4I_{9/2}$ transition of Nd^{3+} which were doped in a pure silicate glass fiber at low temperatures.^{3,4}

If we assume that $\Delta\Gamma_h(T) = AT + BF(T)$ in Figs. 4–6(b), we obtain $A = 300$ MHz/K and $B = 150$ MHz for 590 nm, $A = 220$ MHz/K, and $B = 70$ MHz for 593 nm, and $A = 130$ MHz/K and $B = 260$ MHz for 598 nm. These values fit well with the experimental results. (Below 6 K the agreement between the theory and the experiments is not good at every wavelength.) If the dephasing were governed by the TLS and Raman processes, however, these temperature dependences contradict the commonly observed T^2 temperature dependence at $T > 10$ K.⁷ In addition, the A parameters of this transition of Nd^{3+} in silicate glass fiber are an order of magnitude larger than the A value of the ${}^4F_{3/2}(1)$ - ${}^4I_{9/2}$ transition of Nd^{3+} in silicate glass fiber ($A = 15.8$ MHz/K and $B = 54.9$ MHz at 892.5 nm⁴).

Assuming strain coupling between the Nd^{3+} ions and the TLS's of silicate glass, Huber, Broer, and Golding¹³ estimated the magnitude of the homogeneous width of the ${}^4F_{3/2}(1)$ - ${}^4I_{9/2}$ transition of Nd^{3+} in a silicate glass by the TLS dephasing process. In their calculation, they used the data of the energy shifts occurring when Nd^{3+} :YAG crystal is subjected to hydrostatic pressure.¹⁴ They showed that the homogeneous width is proportional to the energy shift caused by the hydrostatic pressure.¹³ The hydrostatic-pressure-caused energy shifts of the Stark levels of the ${}^4G_{5/2}$, ${}^2G_{7/2}$ - ${}^4I_{9/2}$ transition of the Nd^{3+} :YAG crystal are about three times as large as those of the ${}^4F_{3/2}(1)$ - ${}^4I_{9/2}$ transition.¹⁴ We estimate that the homogeneous width of the ${}^4G_{5/2}$, ${}^2G_{7/2}$ - ${}^4I_{9/2}$ transition by the TLS dephasing process are three times as large as that of the ${}^4F_{3/2}(1)$ - ${}^4I_{9/2}$ transition when dephasing is caused by the TLS dephasing process. The measured A values, however, are an order of magnitude larger than the obtained A value for the ${}^4F_{3/2}(1)$ - ${}^4I_{9/2}$ transition. The absence of T^2 dependence down to 10 K and the larger-than-estimated A values show that the TLS dephasing process and the Raman process with low-frequency modes are not the dominant dephasing mechanisms.

In trying to account for the $\Delta\Gamma_h(T)$ values by the one-phonon process,¹⁰ we use the following equation:¹⁰

$$\Delta\Gamma_h(T) = C / [\exp(\Delta E/kT) - 1], \quad (2)$$

where ΔE is the energy difference between two specific Stark levels, k is the Boltzmann constant and C is a fitting parameter. When determining the C and ΔE values in Eq. (2), we used data also at $T < 6$ K and the inhomogeneous broadening was neglected for simplicity.

The curves in Figs. 4–6(b) were obtained using $C = 4.2$ GHz and $\Delta E = 6.2 \text{ cm}^{-1}$ for 590 nm, $C = 2.2$ GHz and $\Delta E = 4.9 \text{ cm}^{-1}$ for 593 nm, and $C = 2.5$ GHz and $\Delta E = 5.6 \text{ cm}^{-1}$ for 598 nm. Although the Stark-level splittings are not evident in Fig. 2, a similar ΔE value [11 cm^{-1} (Ref. 15)] was obtained from the ${}^4G_{5/2}$, ${}^2G_{7/2}$ - ${}^4I_{9/2}$ transition of Nd^{3+} : LaF_3 crystal. A similar C value ($C = 2$ GHz at $\Delta E = 23 \text{ cm}^{-1}$) has

also been obtained in $\text{Pr}^{3+}:\text{LaF}_3$.⁸ If we assume the Debye model, the rate of phonon emission and absorption scales ω^3 ,¹⁰ where ω is the frequency of phonons. Therefore we expect $C \sim 2 \times (6.2/23)^3 = 0.039$ GHz at 6 cm^{-1} using the value of $\text{Pr}^{3+}:\text{LaF}_3$ and assuming that the density of phonon states are the same for crystals and glasses. Although the scaling is not always applicable (For example, the scaling does not apply well to the data in Table I of Ref. 8.), the larger value than that expected by the Debye model shows that the one-phonon process is caused by the low-frequency modes of silicate glass.

The agreement between the theory and the results of the experiments shows that the dephasing is probably caused by the one-phonon processes between the Stark levels of Nd^{3+} . This kind of dephasing process differs from the often observed dephasing processes of rare-earth ion-doped glasses: the TLS dephasing process and the Raman process with low-frequency modes peculiar to glasses.^{3,4}

Now we consider the possibility of the one-phonon processes of the excited and ground states. In interpreting the previous experiments on accumulated photon echoes for the $^4F_{3/2}(1) \rightarrow ^4I_{9/2}$ transition of Nd^{3+} in a silicate glass fiber between 1.6 and 44 K,⁴ we attributed the dephasing mechanism to the TLS dephasing process and the Raman process with low-frequency modes and excluded the possibility of the one-phonon processes. The magnitude of $\Gamma_h(T)$ of the $^4G_{5/2}$, $^2G_{7/2} \rightarrow ^4I_{9/2}$ transition is larger than that of the $^4F_{3/2}(1) \rightarrow ^4I_{9/2}$ transition⁴ when Nd^{3+} ions are doped in a silicate glass fiber. Therefore the contribution of the one-phonon process in the ground state should be smaller than that in the excited state. We exclude the contribution of the one-phonon processes in the ground state and consider that dephasing is only caused by one-phonon processes between the excited Stark levels at the $^4G_{5/2}$, $^2G_{7/2} \rightarrow ^4I_{9/2}$ transition, at least in the measured temperature regime.

The different dephasing processes between the $^4G_{5/2}$, $^2G_{7/2} \rightarrow ^4I_{9/2}$ transition and the $^4F_{3/2}(1) \rightarrow ^4I_{9/2}$ transition of Nd^{3+} in a silicate glass fiber may be attributed to the differences of the energy-level distributions between the $^4G_{5/2}$ and $^2G_{7/2}$ states (densely distributed states) and the $^4F_{3/2}(1)$ state (single state). Phonon emission and/or absorption in the $^4G_{5/2}$ and $^2G_{7/2}$ states will occur easily because of the narrow distribution of the energy levels.

The dephasing processes of the $^4G_{5/2}$, $^2G_{7/2} \rightarrow ^4I_{9/2}$ transition of Nd^{3+} in an ordered crystal [LaF_3 (Ref. 8)], and a disordered crystal [$\text{CaF}_2\text{-YF}_3$ (Ref. 9)] have already been considered to be the one-phonon processes between the Stark levels of Nd^{3+} . Therefore the dephasing process of the $^4G_{5/2}$, $^2G_{7/2} \rightarrow ^4I_{9/2}$ transition of Nd^{3+} is considered to be determined by the one-phonon processes between the Stark levels of Nd^{3+} regardless of the disorder of the inorganic host material (crystal or glass).

Figure 7 shows the transition-wavelength dependences of the homogeneous widths $\Gamma_h(4.2 \text{ K})$ and $\Gamma_h(T \rightarrow 0)$. The boxes show values obtained at 4.2 K, and the circles show the temperature-independent homogeneous width $\Gamma_h(T \rightarrow 0)$. Both $\Gamma_h(4.2 \text{ K})$ and $\Gamma_h(T \rightarrow 0)$ are smaller at longer wavelengths. At 596 and 598 nm, the measured homogeneous widths are temperature independent at $T \leq 2.5 \text{ K}$, and are the same value. As the transition-wavelength decreases, the homogeneous width becomes temperature independent at

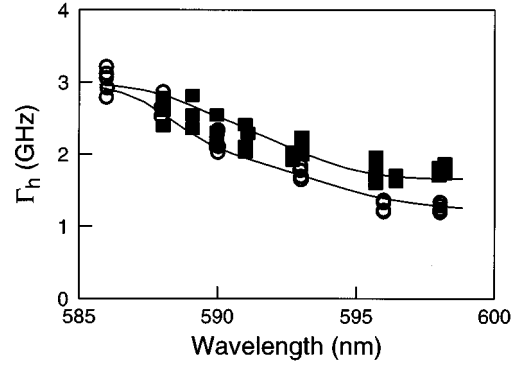


FIG. 7. Measured homogeneous widths as a function of transition wavelength. Boxes show $\Gamma_h(4.2 \text{ K})$ and circles show $\Gamma_h(T \rightarrow 0)$. The curves are theoretical curves for the one-phonon process model with the upper one for 4.2 K and the lower one for 1.6 K.

higher temperatures. The homogeneous width at 588 nm is temperature independent at $T \leq 4.2 \text{ K}$. A similar tendency has been observed in the transition-wavelength dependence of the homogeneous width measured for $\text{Nd}^{3+}:\text{ED-2}$ silicate glass.¹²

This dependence can be explained qualitatively by the one-phonon process in the following way. Assume that the energy splittings of the Stark levels which contribute to the dephasing increase as the wavelength is decreased. We then expect that the homogeneous width will be temperature independent at higher temperatures when the transition-wavelength decreases. And if the parameter C becomes larger at shorter wavelengths, the overall transition-wavelength dependence shown in Fig. 7 can be well understood.

The transition-wavelength dependence of the homogeneous widths shown in Fig. 7 can be explained numerically in the following way. The energy of the j th Stark level is given by E_j and E_1 is set to 0. The energy difference between the j th and k th Stark levels is given by ΔE_{jk} ($=\Delta E_{kj}$). For simplicity we consider only one-phonon processes between adjacent levels ($j \leftrightarrow j \pm 1$). The $^4G_{5/2}$ and $^2G_{7/2}$ Stark levels are Kramers' degenerate levels and show at most seven levels,¹⁷ so here we consider seven levels.

The homogeneous width $\Gamma_{hj}(T)$ between the j th excited Stark level and the ground state is given by¹⁰

$$\Gamma_{h1}(T) = A_{12}N(\Delta E_{12}) + A_0, \quad (3)$$

$$\Gamma_{hj}(T) = A_{jj+1}N(\Delta E_{jj+1}) + A_{jj-1}\{N(\Delta E_{jj-1}) + 1\} \quad (j=2 \text{ to } 6), \quad (4)$$

and

$$\Gamma_{h7}(T) = A_{76}\{N(\Delta E_{76}) + 1\}, \quad (5)$$

where

$$N(\Delta E_{jj+1}) = 1/\{\exp(\Delta E_{jj+1}/kT) - 1\}, \quad (6)$$

$$A_{jk} = A_{kj}, \quad (7)$$

and A_0 is the lifetime contribution of the first Stark level at $T \rightarrow 0$. The inhomogeneous widths of all the Stark levels are assumed to be the same and are set to ω_{inh} .

The echo signal $E_{\text{echo}}(t_{12})$ induced from the population grating by the pump beam E_1 is given by^{19,20}

$$E_{\text{echo}}(t_{12}) \propto \sum_j P_j^4 W_j(\omega_L) \exp[-2\pi\Gamma_{hj}(T)t_{12}], \quad (8)$$

where P_j is the electric dipole moment between the j th excited Stark level and the ground state. $W_j(\omega_L)$'s ($j=1-7$) are weight functions which take into account of the inhomogeneous broadening, and are given by

$$W_j(\omega_L) = \exp\{-4(\ln 2)(\omega_L - E_j/h)^2/\omega_{\text{inh}}^2\}. \quad (9)$$

Here ω_L is the laser frequency measured from the center of the first excited-state Stark level. The spectral width of the exciting laser is assumed to be much smaller than ω_{inh} . Since the spectral width of the laser was about 10 cm^{-1} and the typical inhomogeneous widths of rare-earth ion-doped glasses are of the order of 100 cm^{-1} ,¹⁸ this assumption is considered to be satisfied. The measured homogeneous width $\Gamma_h(\omega_L, T)$ is given by assuming Eq. (8) to be a single exponential decay curve proportional to $\exp[-2\pi\Gamma_h(\omega_L, T)t_{12}]$.

Because the Stark levels of Nd^{3+} in a silicate glass fiber have not been measured, we must assume the values for the Stark-level splittings. Using the Stark levels of $\text{Nd}^{3+}:\text{ED-2}$ silicate glass¹² and $\text{Nd}^{3+}:\text{LaF}_3$ crystal¹⁵ as references, we tentatively set the Stark-level splittings from the lowest one as 5.6, 70, 80, 6.2, 190, and 200 cm^{-1} and tried to fit the data plotted in Fig. 7.

The curves shown there are obtained by using the following parameters: $A_0=0.80 \text{ GHz}$, $A_{12}=2.5 \text{ GHz}$, $A_{23}=1.5 \text{ GHz}$, $A_{34}=1.6 \text{ GHz}$, $A_{45}=3.3 \text{ GHz}$, $A_{56}=3.1 \text{ GHz}$, $A_{67}=8.3 \text{ GHz}$, and $\omega_{\text{inh}}=170 \text{ cm}^{-1}$. The center of the transition wave-

length of the first Stark level was set to be 598 nm. The temperatures were set to be 1.6 K for the lower curve and 4.2 K for the upper curve. For simplicity, the P_j 's were set to be the same for all j 's. Although the ΔE_{jj+1} values are tentative, the whole transition-wavelength dependence of the homogeneous widths are well explained by the one-phonon process model. If we assume that $\omega_{\text{inh}} > 220 \text{ cm}^{-1}$ or $\omega_{\text{inh}} < 130 \text{ cm}^{-1}$, the agreement becomes worse even if we change both the A_{jj+1} and ΔE_{jj+1} parameters. As the inhomogeneous widths of the $^5D_0-^7F_0$ transition of Eu^{3+} in a silicate fiber³ and the $^4F_{3/2}(1)-^4I_{9/2}$ transition of Nd^{3+} in a silicate glass fiber⁴ are, respectively, about 240 cm^{-1} and about 80 cm^{-1} , the assumed value of 170 cm^{-1} is considered to be not far from the true value.

IV. CONCLUSION

The temperature dependence of the homogeneous width of the $^4G_{5/2}-^4I_{9/2}$ transition of Nd^{3+} in a pure silicate glass fiber measured between 1.5 and 44 K by using accumulated photon echoes cannot be explained by the TLS dephasing process and the Raman process with low-frequency modes peculiar to glasses. The dominant dephasing process is instead considered to be one-phonon processes between the Stark levels of Nd^{3+} as in the case of ordered and disordered crystals. The densely distributed Stark levels of the $^4G_{5/2}$ and $^2G_{7/2}$ states are responsible for these one-phonon processes. Our experimental results show that the dephasing process of this transition is considered to be independent of the disorder of the inorganic host material (crystal or glass) and to be governed by one-phonon processes. The transition-wavelength dependences of the homogeneous widths $\Gamma_h(4.2 \text{ K})$ and $\Gamma_h(T \rightarrow 0)$ are explained well by using the one-phonon process model.

- ¹*Optical Spectroscopy of Glasses*, edited by I. Zschokke (Reidel, Dordrecht, 1986); *Persistent Spectral Hole-Burning: Science and Applications*, edited by W. E. Moerner, Topics in Current Physics Vol. 44 (Springer-Verlag, Berlin, 1988).
- ²W. H. Hesselink and D. A. Wiersma, Phys. Rev. Lett. **43**, 1991 (1979).
- ³R. Yano, N. Mitsunaga, N. Uesugi, and M. Shimizu, Phys. Rev. B **50**, 9031 (1994).
- ⁴R. Yano and N. Uesugi, Opt. Commun. **119**, 545 (1995).
- ⁵D. H. Huber, J. Lumin. **36**, 327 (1987).
- ⁶*Amorphous Solids: Low-Temperature Physics*, edited by W. A. Phillips, Topics in Current Physics Vol. 24 (Springer-Verlag, Berlin, 1981).
- ⁷P. M. Selzer, D. H. Huber, D. S. Hamilton, W. M. Yen, and M. J. Weber, Phys. Rev. Lett. **36**, 813 (1976).
- ⁸T. Kohmoto, H. Nakatsuka, and M. Matsuoka, Jpn. J. Appl. Phys. **22**, L571 (1983).
- ⁹K. W. Ver Steeg, A. Ya. Karasik, R. Reeves, and T. T. Basiev, J. Lumin. **60&61**, 742 (1994).
- ¹⁰B. Di Bartolo, *Optical Interactions in Solids* (Wiley, New York,

- 1968).
- ¹¹H. W. H. Lee, L. Lumin. **45**, 99 (1990).
- ¹²R. M. Shelby, Opt. Lett. **8**, 88 (1983).
- ¹³D. L. Huber, M. M. Broer, and B. Golding, Phys. Rev. Lett. **52**, 2281 (1984).
- ¹⁴V. A. Voloshin, L. A. Ivchenko, M. G. Krimus, and V. P. Kondratenko, Zh. Prikl. Spektrosk. **26**, 353 (1977) [J. Appl. Spectrosc. (USSR) **26**, 267 (1977)].
- ¹⁵H. H. Caspers, H. E. Rast, and A. Buchanan, J. Chem. Phys. **42**, 3214 (1965).
- ¹⁶U. Buchenau, N. Nücker, and A. J. Dianoux, Phys. Rev. Lett. **53**, 2316 (1984), **56**, 539 (1986).
- ¹⁷R. M. Macfarlane and R. M. Shelby, in *Spectroscopy of Solids Containing Rare Earth Ions*, edited by A. A. Kaplyanskii and R. M. Macfarlane (North-Holland, Amsterdam, 1987).
- ¹⁸R. M. Macfarlane and R. M. Shelby, J. Lumin. **36**, 179 (1987).
- ¹⁹S. Asaka, H. Nakatsuka, M. Fujiwara, and M. Matsuoka, Phys. Rev. A **29**, 2286 (1984).
- ²⁰M. Mitsunaga, R. Yano, and N. Uesugi, Phys. Rev. B **45**, 12 760 (1992).